



Wear in wind turbine pitch bearings—A comparative design study

Fabian Schwack^{1,2}  | Fabian Halmos³ | Matthias Stammler⁴  | Gerhard Poll² | Sergei Glavatskih^{1,5,6} 

¹Department of Machine Design, KTH Royal Institute of Technology, Stockholm, Sweden

²Institute of Machine Design and Tribology, Leibniz University Hannover, Hannover, Germany

³Engineering Design, Friedrich-Alexander-Universität Erlangen-Nürnberg (FAU), Erlangen, Germany

⁴Department of Reliability and Validation, Fraunhofer Institute for Wind Energy System, Hamburg, Germany

⁵Department of Electromechanical, Systems and Metal Engineering, Ghent University, Ghent, Belgium

⁶School of Chemistry, University of New South Wales, Sydney, New South Wales, Australia

Correspondence

Fabian Schwack, Department of Machine Design, KTH Royal Institute of Technology, Stockholm, Sweden.
Email: schwack@kth.se

Present Address

Brinellvägen 83, SE-10044 Stockholm, Sweden

Funding information

German Federal Ministry of Economic Affairs and Energy (BMWi), Grant/Award Number: 0325918

Abstract

We tested two types of ball bearings with an outer diameter of 750 mm to learn more about the challenges of oscillating motions for pitch bearings. The experimental conditions are derived from aero-elastic simulations, long-term wind speed measurements and a scaling method that considers loads and pitch angles. As a result, the parameters relevant for pitch bearings are represented appropriately, and the findings are transferable to other bearing sizes. For the tested parameter sets, severe wear occurred for over 90% of the exposed contact areas after 12 500 oscillating cycles. Decreasing the number of cycles to 1250 leads to a mix of exposed areas with 13% severe wear, 32% mild wear and 55% no wear, with no apparent pattern. The results demonstrate that a comparatively small amount of consecutive cycles can lead to severe wear. A new type of bearing tested showed less wear for the selected operating conditions.

KEYWORDS

bearing design, blade bearing, downscaled experiments, individual pitch control

1 | INTRODUCTION

Modern wind turbines use pitch control to limit their power output and aerodynamic loads.¹ The blades of the wind turbine change their aerodynamic angle of attack with the wind speed. For further load reduction, pitch mechanisms of modern turbines control each blade individually and continuously.^{2,3} A schematic representation of pitch control's influence on power output, rotational speed and loads can be seen in Figure 1. The blade's needed pivoting movement is facilitated by a bearing that connects the rotor hub and the blade.¹ The requirement of lots of starts and stops, centrifugal forces from the rotating hub and as little maintenance as possible lead to the use of grease lubricated rolling element bearings.⁴ From a tribological point of view, oscillating movements, as they occur in pitch bearings, are unsuitable for rolling bearings. The oscillating motions, both small and large, can lead to wear,^{5–8} especially for bearings lubricated with grease.^{9,10} The use of individual continuous pitch

This is an open access article under the terms of the Creative Commons Attribution-NonCommercial License, which permits use, distribution and reproduction in any medium, provided the original work is properly cited and is not used for commercial purposes.

© 2021 The Authors. *Wind Energy* published by John Wiley & Sons Ltd.

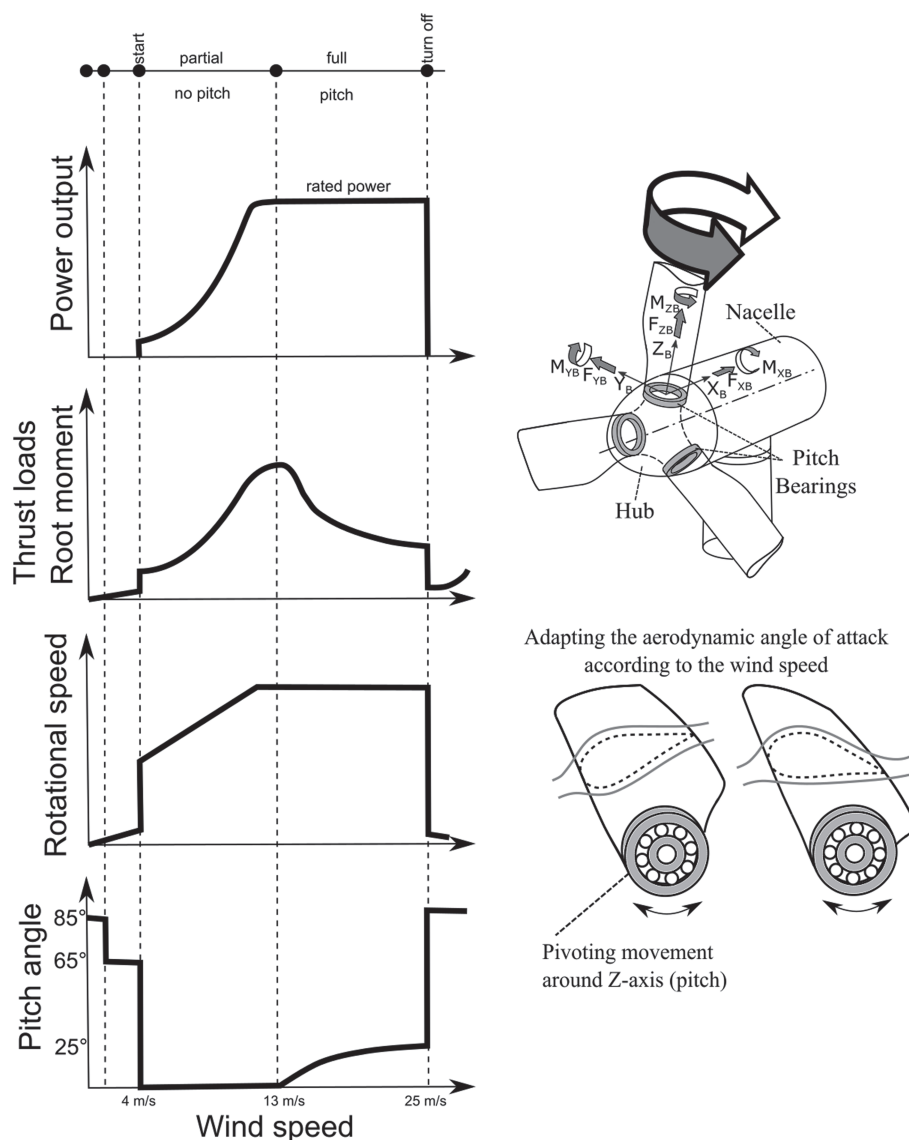


FIGURE 1 Schematic representation of the control strategy. The relation of power output, loads, rotational speed and pitch angle to the wind speeds is shown qualitatively to the left. The coordinate system and the pivoting movement of the pitch bearing are shown to the right

controllers^{2,3} often leads to more cycles, starved lubrication and increased risk of wear and more pronounced wear.¹¹ Nevertheless, some individual pitch controllers may positively affect the bearings since the pitch sequences are more favourable.^{12,13}

Experiments on wind turbine pitch bearings on a full scale are very time-consuming and costly. However, there are examples of investigations of pitch bearings and large-scale slewing bearings. Chaib et al. focused on the screw behaviour in large slewing bearings.¹⁴ The experimental results are based on a bearing with outer diameter of 695 mm. The test rig for pitch and yaw bearings described by Nam et al. is capable of testing different load conditions for bearings up to an outer diameter of 3500 mm.¹⁵ This test rig was used by Han et al. to investigate fatigue life of pitch bearings.¹⁶ Similar investigations were performed by He et al. for bearing with an outer diameter of 811 mm. Liu et al. used slewing bearings with an outer diameter of 1122 mm for experimental verification of load simulations.¹⁷ Stammer et al. used the pitch drive of a 3-MW-call pitch bearing with 2.3-m diameter to compare friction torque models with measurements.¹⁸ The influence of the contact angle on raceway fretting was investigated by He et al. on pitch bearings with an outer diameter of 1200 mm.¹⁹ They only used parts of the bearing raceway. None of the studies mentioned include wear due to oscillating motion and different bearing designs. Stammer et al. dealt with a strategy for accelerated pitch bearing tests.¹³ Investigations were carried out on the original scale and included wear tests. A 7.5-MW turbine was used as a reference.²⁰ The tested pitch bearings were four-point bearings with an outer diameter of 5000 mm.

Most conclusions on wind turbine pitch bearings' operational behaviour are drawn based on tested bearings with diameters around 100 mm and smaller. A considerable amount of literature deals with lubrication in oscillating bearings. As early as 1937, different grease lubricants were tested under oscillating conditions.⁵ Comparison of different lubricants for oscillating conditions can also be found in modern literature.²¹⁻²⁴ Next

to this, different studies on wear in oscillating bearings exist. Often a specific lubricant is examined, and the sensitivity of a certain parameter, such as the frequency, the number of cycles or the oscillation angle, is examined. Noteworthy examples are previous studies.^{25–30} No parameter can be derived from the literature that generally dominates. With the help of simulations, we examined various parameters⁸ and analysed the frictional energy for different oscillation angles³¹ for angular contact ball bearings. In addition to experiments on bearings, model tests such as the SchwingungsReibverschleiß-Prüfgerät (SRV) are often used to investigate lubrication and wear in a controlled environment.³² Due to the pure sliding movement in the experiment, the results are sometimes difficult to transfer to rolling element bearings.³³

Rolling contact fatigue in oscillating rolling element bearings is also an essential factor. However, mostly wear dominates. Fatigue calculation approaches for oscillating bearings differ from approaches for rotating bearings.^{16,34,35} In addition, there is currently no standardized approach. Dependent on the operating conditions, the different approaches deliver different results.^{36–38}

However, not all operating parameters of these studies match the conditions to which wind turbine pitch bearings are exposed. From the literature on oscillating bearings, it can be summarized that wear is a significant problem, influenced by the chosen lubricant and the operating conditions. Even lubricants with properties suitable for oscillating bearings cannot prevent wear at a constant oscillation amplitude, but they can reduce wear.

This paper presents experimental results for wind turbine pitch bearings with an outer diameter of 750 mm. The test bearings were scaled down from a pitch bearing for a 7.5-MW reference turbine³⁹ and were manufactured by the bearing company IMO under the quality standards of Germanischer Lloyd.⁴⁰ For the experiments, a test rig applies static axial loads and oscillating movements. From aero-elastic simulation and cycle analysis and wind speed measurements, we selected two parameter sets for the experiments, 0.7° and 3.0° both at 2-GPa maximum contact pressure and 12 500 oscillating cycles. The test parameters represent typical operating conditions of wind turbine pitch bearings and can be easily transferred to different bearing sizes. Two different bearing designs are part of the study. The analysis focuses on the occurring wear and its distribution along the raceway circumference.

2 | BEARING DESIGN

The type of pitch bearings depends on the overall wind turbine system. Pitch bearing costs depend on the type, design and dimensions and can be estimated using the rotor diameter.⁴¹ Four-point contact ball bearings are state of the art for multi-megawatt wind turbines.¹ Four-point bearings are angular contact ball bearings that can withstand bending moments and axial loads in both directions. For modern wind turbines, the load carrying capacity of single-row four-point bearings is usually not sufficient. Therefore, two-row four-point bearings are commonly used.³⁴ Figure 2 shows schematically the cross-sections of four-point contact ball bearings. It shows exemplary one and two-row designs with a spur gear. Alternatives to gears are hydraulic pistons and belt drives.

Alternative designs have dedicated rolling element rows for axial and radial loads. The blade's bending moments translate to a distribution of axial loads along the circumference of the blade root. These axial loads are the dominating forces in a pitch bearing. Figure 3 shows two approaches.

Another possibility are roller bearings; see Figure 4. Roller bearings are known to have larger loading capacity but also higher costs compared to ball bearings.⁴² One of the cheapest roller bearings is the crossed roller bearing; see Figure 4 (left). In this bearing, the rollers are alternately crossed so that axial loads in both directions are possible. The disadvantage is the high slip on the end faces as well as wear from roller sliding. Another alternative are three-row cylindrical roller bearings; see Figure 4 (right). These enable high axial loads to be accommodated in both directions. In addition, the required transfer of the bending moments is possible for both described bearing designs.

Another design that is rarely used as a pitch bearing due to the comparably high friction on the flanges are tapered roller bearings. Nevertheless, the load carrying capacity is comparably high, and no spin slip occurs in these bearings.

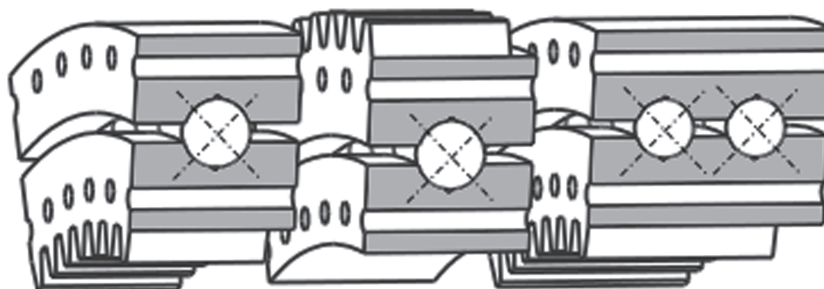


FIGURE 2 Examples of four-point contact ball bearings for the use as wind turbine pitch bearing

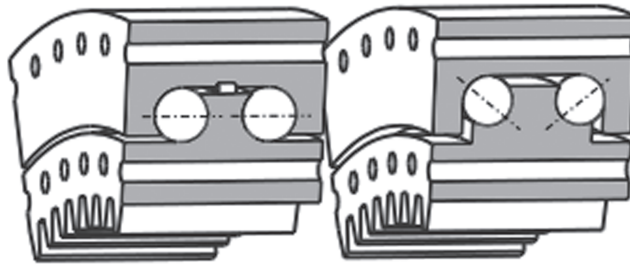


FIGURE 3 Ball bearings with special rolling element arrangement for improved stiffness behaviour and load accommodation

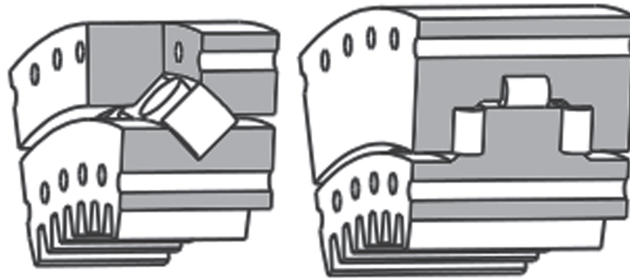


FIGURE 4 Cylindrical roller bearing for the use as wind turbine pitch bearing

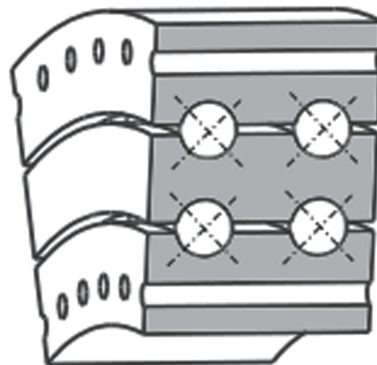


FIGURE 5 Schematic representation of a multi-ring bearing

The concept of multi-ring bearings is also possible; see Figure 5. The idea is to have one ring continuously moving, to avoid damages from small oscillations. This design is associated with higher costs, more space and lower stiffness values.

Juettner et al. as well as the bearing manufacturer SKF present the idea of a bearing concept, which for small oscillating amplitudes exploits the bending stiffness of lamellas and for large ones uses a segmented plain bearing.^{43,44} This could prevent wear caused by micro-oscillations. However, the actual installation space and the weight of such bearing are significantly higher compared to conventional pitch bearings.

3 | TEST BEARINGS

The study focuses on four-point contact ball bearings, as they are currently the most common wind turbine pitch bearings. The bearings are manufactured in accordance with international standards.⁴⁰ The downscaled experimental bearings with a pitch diameter of around 675 mm could as well be used for real applications in small wind turbines. The design and the scaled dimensions of the bearings are based on a reference pitch bearing, the first design of this is described in Schwack et al,⁴⁵ a later evolution in Stammler et al.¹³ We made the bearings as small as possible while using the same manufacturing process and keeping all the special features of pitch bearings. In addition to the four-point contact ball bearing, we investigate a so-called T-Solid, which design is supposed to protect the bearing rings against excessive deformation.^{46–48} A comparison of the two bearing types is purely qualitative since a quantitative result through repeated tests is not within the research scope. Main differences

between the bearing types are the initial contact angle and the osculation. The initial contact angle of the four-point contact bearing is 45° and 90° for the T-Solid. In order to achieve the same contact pressure in both bearings, the number of rolling elements in the experiments is reduced for both bearing designs. If the osculation of both bearings is approximated, the T-Solid has an approximately 5% closer osculation than the four-point bearing. Due to our experimental approach, the initial contact angle has no direct influence on the load, but indirect influences can arise from deformations. Larger contact angles lead to higher spin slip,^{49,50} which increases the frictional work, and therefore can increase wear risk.⁸ However, the larger the diameter of the bearing, the smaller the impact of the spin slip on frictional work. The osculation influences the contact pressure, but since the contact pressure in both bearings is the same, this influence is not relevant for the experiments. Closer osculations provide better guidance behaviour but lead to higher differential slip, which can increase the risk of wear.^{8,51}

3.1 | Four-point contact ball bearing

The cross-sectional view of the four-point contact ball bearing can be seen in Figure 6A. The 3D view is shown in Figure 6B. Table 1 lists the bearing dimensions. To reach a higher contact pressure during the experiments, these bearings have a reduced number of 28 rolling elements. The bearing rings are made of 42CrMo4. The initial lubrication of the bearing is accomplished through the lubrication inlets on the outer ring. The bearing is rotated to ensure grease distribution. A picture of the bearing raceway is shown in Figure 7.

3.2 | T-Solid bearing

Four-point bearings with insufficient internal or external stiffness are prone to truncation. Truncation occurs when a large deformation of the bearing rings extends the contact area of ball and raceway over the edge of the raceway. That the risk of truncation for the four-point contact ball bearing of the reference turbine is given was demonstrated by Schwack et al.³⁶

The major difference between the T-Solid and the four-point contact ball bearing is the arrangement of the rolling elements. The axial rows of the T-Solid have a contact angle of nearly 90° . Figure 8 shows a cross-sectional view and a 3D view. The t-shaped outer ring coined the name for this bearing type. Another feature is the split inner ring, which allows a faster assembly process than filling the rows by fill plugs. The radial

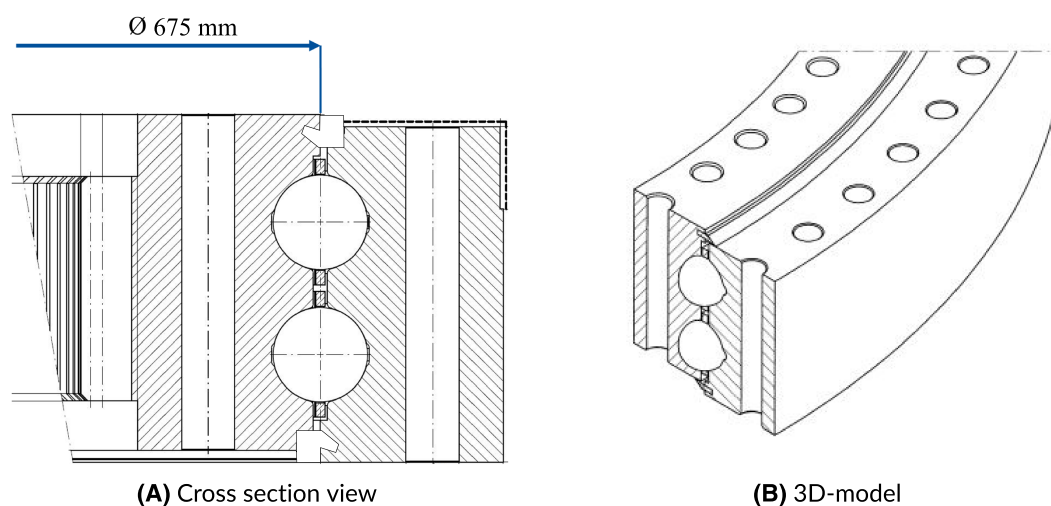


FIGURE 6 Four-point contact ball bearing

TABLE 1 Properties of four-point contact ball bearing

Parameter	Value
Pitch diameter D_p	675 mm
Outer diameter D_o	750 mm
Rolling element diameter D_{RE}	20 mm
Rolling elements	84 (28) per row



FIGURE 7 Inner ring raceways of the four-point bearing

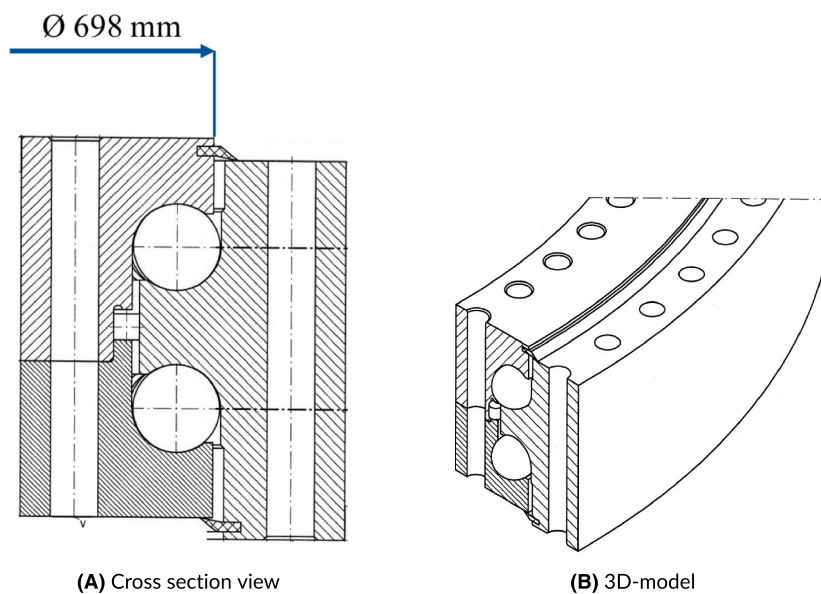


FIGURE 8 T-Solid bearing

TABLE 2 Properties of T-Solid bearing

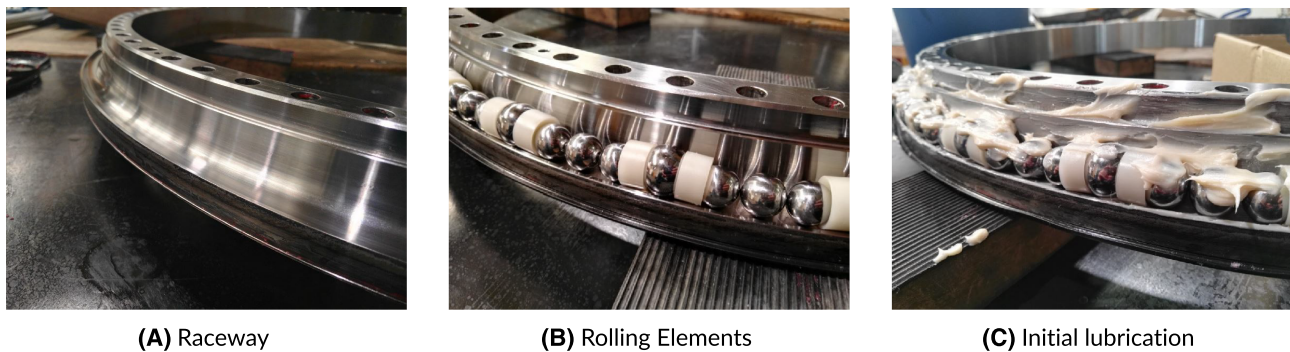
Characteristic	Value
Pitch diameter D_p	672 mm
Outer diameter D_o	750 mm
Rolling element diameter D_{RE}	20 mm
Rolling elements	95 (29) per row

loads are completely transferred by cylindrical rollers. Thus, the arrangement is optimized for the axial loads and bending moments that dominate the load situation.⁵²

The dimensions of the the T-Solid test bearing are given in Tables 2 and 3. The osculation of the T-Solid is tighter, and the number of rolling elements is higher. It is worth mentioning that due to the geometry of the T-Solid, fewer contact spots occur under purely axial loads. The radial raceway, dimensions given in Table 3, is not loaded under pure axial loads and will therefore be not further investigated. The number of rolling elements will be reduced to 29 for the T-Solid, to reach a higher maximum contact pressure. The rolling element reduction is realized by spacers

TABLE 3 Properties of T-Solid bearing—Radial raceway

Characteristic	Value
Pitch diameter D_p	655 mm
Rolling element diameter and length	6 and 6 mm
Rolling elements	339

**FIGURE 9** Raceway, rolling elements, mounting and initial lubrication of T-Solid bearing

and smaller balls, which are shown in Figure 9. Figure 9A shows the raceway without rolling elements. Three smaller balls secure the distance between two carrying rolling elements, Figure 9B. The initial lubrication is done during the assembly; see Figure 9C. This allows for a more uniform distribution of grease than filling through inlets.

4 | DATA AND DOWNSCALING

Amplitude and sequences of oscillations have a major influence on the occurrence of wear. Any constant oscillation causes wear in a bearing if the number of cycles is high enough.¹¹ Stammler et al. showed that longer movements that interrupt sequences of short oscillations can prevent wear.¹² These movements are called protection runs. In their work,¹³ Stammler et al. showed that a double amplitude (peak-to-peak amplitude) of 5° is not enough to prevent wear on the pitch bearings of the reference turbine. Later endurance run results showed a double amplitude of 15° is an effective protection run. Since further test results are currently not available, the double amplitude for an effective protection run is assumed to be larger than 5° .

The experiments in this work aim at reflecting wind turbine conditions. In order to find a suitable number of cycles for the tests, we combine simulation data of the reference turbine²⁰ and wind speed measurements. The wind speed measurements are LiDAR measurements at a height of 119 m, the hub height of the reference turbine. The measurement data are from a nearshore location at the North Sea, covers one full year and has a sample rate of 10 min. It contains both average and maximum wind speeds.

Since the oscillation characteristics of pitch bearings vary largely over time,^{12,13} it is necessary to find the longest duration with constantly critical operating conditions to derive cycles for a wear test. Critical conditions are where the double amplitude does not exceed 5° . Figure 10 shows the simulated pitch angles over wind speed.

The green dots are all data points, whereas the orange dots mark the pitch angles for all situations where the instantaneous wind speed is equal or higher than the mean wind speed of the simulation file -2 m/s. This filter respects the behaviour of the turbine controller that reacts to sudden wind speed changes as a delaying low pass filter. If the mean wind speed is rather high, so is the overall pitch angle, and the turbine needs time to react to a drop in wind speed. This explains situations with a relatively high pitch angle and relatively low speed. Since we are looking at situations with a rather low wind speed to find the longest possible period with small oscillations, we omit these situations from the following analysis and continue with the orange data points. Figure 11 shows the maximum detected pitch angle, again for situations where the current wind speed is equal or higher than average -2 m/s. This confirms that effective protection runs in the simulation do not occur at wind speeds at or below 10 m/s.

We applied this threshold from the simulation data to the measurement data and filtered it for the longest consecutive period below or at exactly 10 m/s maximum wind speed and at or above 3 m/s mean wind speed; 3 m/s is the cut-in wind speed of the turbine. This period is 41.5 h and is the longest duration the turbine operated continuously below 10 m/s. To understand the characteristics of oscillations during these

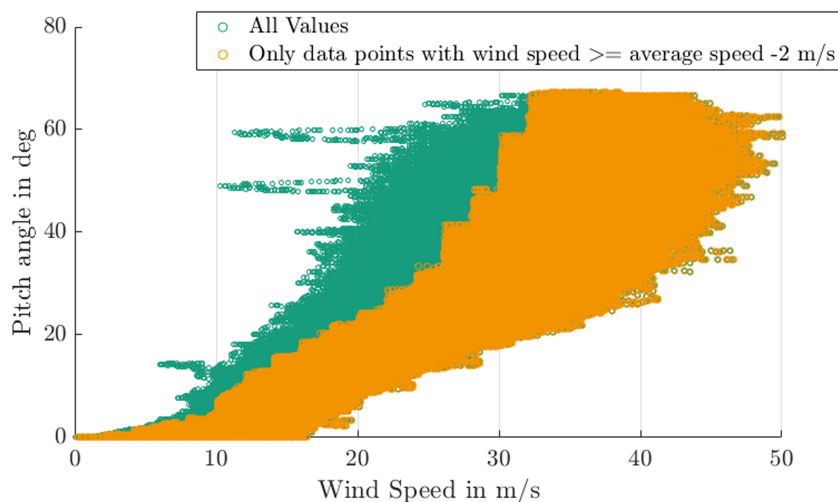


FIGURE 10 Simulated pitch angles over wind speed for all load cases

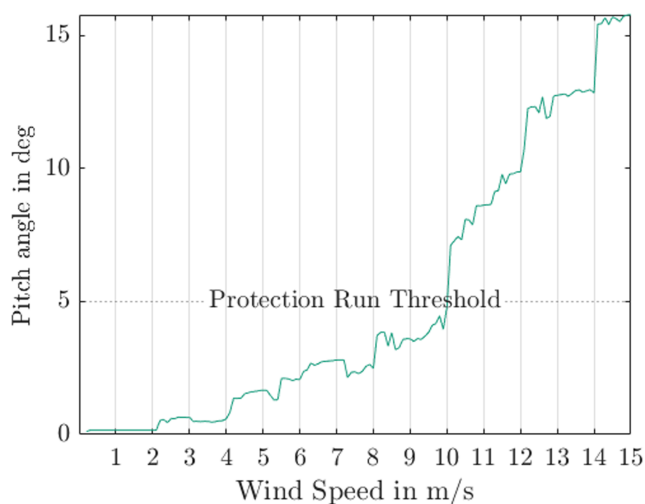


FIGURE 11 Maximum simulated pitch angles over wind speed and protection run threshold

conditions, the simulation data were cleared of any data files with a mean wind speed above 10 m/s and below 3 m/s. A cycle count (see Stammler et al.⁵²) of the resulting data set returned pitch activity (actuator duty cycle, ADC) for 60.33% of the time with the bulk of cycles being below 1° travel. The average frequency of the pitch cycles is 0.153 Hz. In 60.33% of 41.5 h, 13 818 cycles occur. This number is connected to some uncertainty, as the underlying data consisted of wind measurements for only 1 year and did not contain minimum wind speeds. However, it gives a good idea of a realistic number of wear-critical cycles the reference turbine can do continuously. The pitch rate or ADC of 60.33% is also close to the overall ADC of the turbine with 59.2% or 98 011 h, which further indicates the operational conditions are not uncommon for this turbine.

A pitch bearing is subject to large bending moments which result in individual ball loads ranging from zero to a peak load throughout the circumference. Tests with large bearings showed clear wear results at a contact pressure of 2 GPa.¹³ Operational loads can reach up to 3 GPa, and higher loads are usually avoided in the design phase.

The scaling of the loads and kinematics is based on the movement x of a rolling element in relation to the double width $2b$ of the HERTZ'ian contact area.⁵³ This dimensionless approach makes it possible to investigate similar operating conditions at different scales and generalize the results. The approach is common for dimensionless investigations of contacts of various sizes. Figure 12 shows the $x/2b$ ratio for two double amplitudes of a bearing for a 7.5-MW turbine and 2-GPa contact pressure. Furthermore, a schematic representation for two bearing sizes and constant $x/2b$ for both is shown. A detailed explanation and mathematical derivation of the scaling procedure for bearings can be found in Schwack et al.¹⁰ The investigations with this scaling approach show good agreement over different scales.

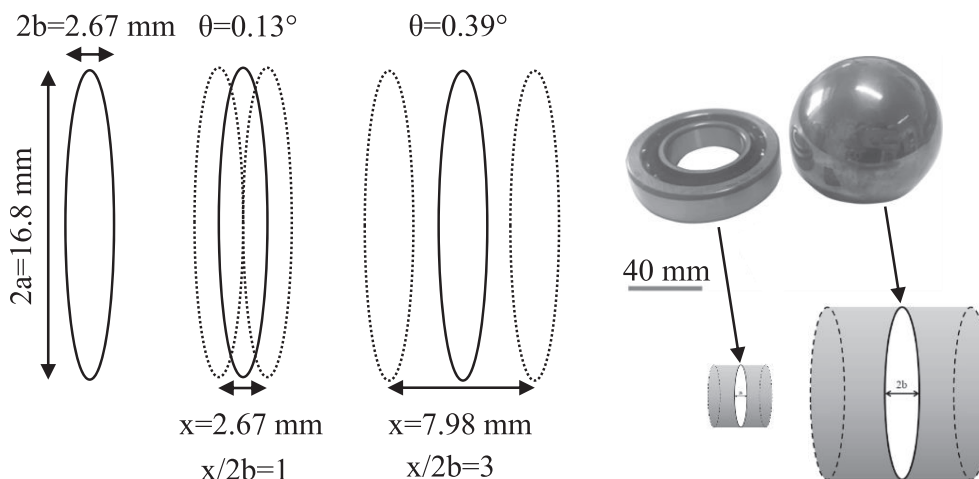


FIGURE 12 $x/2b$ scaling examples based on published data¹³ and a schematic representation for two bearing sizes

TABLE 4 Test parameters

Bearing type	$x/2b$	Cycles N
Four-point	2.67	12 500
Four-point	11.44	12 500
Four-point	2.67	1250
T-Solid	2.67	12 500
T-Solid	11.44	12 500

5 | EXPERIMENTAL APPROACH

The test plan (see Table 4) comprised five individual tests. The parameters differ mainly in the double oscillating amplitude θ that was chosen to be 0.7° ($x/2b = 2.67$) and 3.0° ($x/2b = 11.44$). These values are typical for modern wind turbine pitch bearings^{10,36,54,55} and can be reproduced with the test bench.

In the following sections, we will only refer to the ratio $x/2b$. The number of cycles for four of the tests was 12 500. This is close to the 13 818 found in the investigations of simulation data and wind speed and still allowed to finish each test within one working day. The highest number of consecutive cycles without interruption is used since this number is critical with view on wear development. To investigate the earlier stages of wear development in common pitch bearing conditions, we additionally tested $x/2b = 2.67$ with 1250 cycles. The oscillating frequency of 0.5 Hz was kept constant for all the experiments. Both bearing types were tested under a maximum contact pressure of 2 GPa, which represents typical pitch bearing operating conditions.^{10,13,36,54,55} Due to the different contact geometry and contact angle of the bearing types and the adapted number of rolling elements for each type, the same axial load was applied for both bearings to reach 2 GPa. As the test duration was limited, there was no re-lubrication of the bearings during the tests.

After the experiments, the bearings were disassembled and cleaned for post-analyses. The wear marks were analysed with a microscope. Therefore, the bearing was cut like shown in Figure 13.

Figure 14 shows the test rig. Per experiment, two bearings are tested at the same time. The bearings were mounted horizontally and oscillated by an electric motor. Hydraulic cylinders applied axial loads. The test rig was equipped with the following sensors:

- 10 displacement transducers
- 2 temperature sensors
- 2 pressure transducers
- 1 torque load cell

All bearings run with a commercial grease that is commonly used in pitch bearings. Table 5 lists its properties as per the data sheet of the manufacturer.

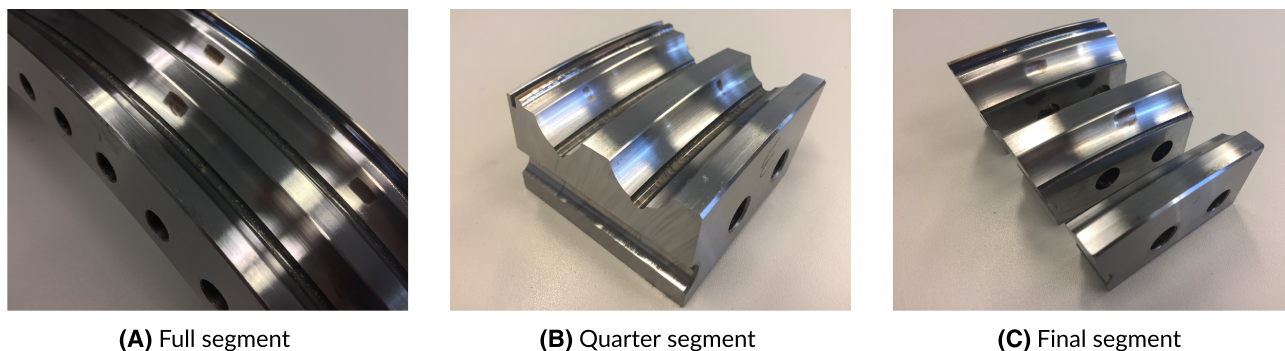


FIGURE 13 Preparation of large bearing for post-analyses

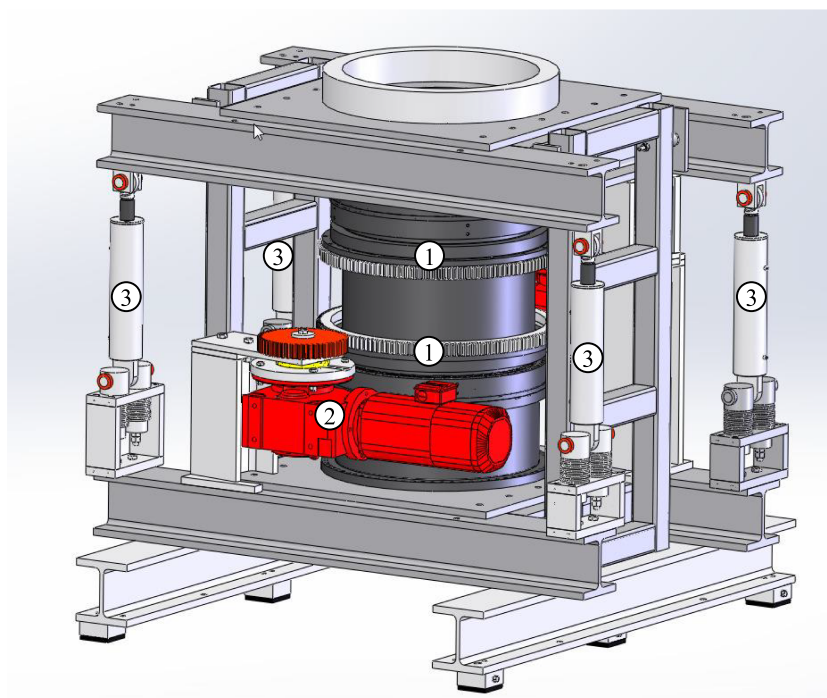


FIGURE 14 3D model of used experimental setup. (1) Test bearings, (2) electric motor and (3) hydraulic cylinders

TABLE 5 Grease properties

NLGI	2
Thickener	Lithium
Base oil viscosity (40°C)	50 mm ² /s
Base oil	Synthetic

6 | RESULTS

Oscillating tests usually result in wear damage of the raceways and/or rolling elements. Due to the small double oscillating amplitudes, contact regions of different rolling bodies do not overlap and wear appears in form of individual wear patches. The raceway areas, which are in contact with the rolling element during the oscillation, are defined as exposed areas. We decided on this definition to create differentiation to the contact area according to Hertz and to emphasize that these areas can be exposed by wear. The degree of damage can vary in shape and reaction products. Each exposed area was analysed with a microscope. We divided the surface conditions of the exposed areas into three classes.

- Severe wear
- Mild wear
- No wear

Severe wear/badly damaged are signs of wear in which over 50% of the contact surface is clearly damaged. Damage of this class shows clear deposits of the reaction product hematite, which indicates direct contact between the rolling element and the raceway. Examples are shown in Figure 15.

The term **mild wear/little damage** refers to wear phenomena whose contact surface is more than 5% and less than 50% damaged. Examples are shown in Figure 16.

The four-point contact ball bearing contains 28 rolling elements per row. Under pure axial load, the raceways have $28 \cdot 4 = 112$ contact areas. The axial rows of a T-Solid only have one active direction; hence, the raceways have $29 \cdot 2 = 58$ contact areas. The loads on each rolling element are almost identical, and this should result in an equally similar visual appearance of the exposed areas. In order to be able to draw conclusions about different degrees of damage, the positions of the damage are analysed.

6.1 | Analyses: Four-point contact ball bearing

Figure 17 shows the distributions of damage classes for $x/2b = 2.67$ and $N = 12500$ of the four-point contact ball bearing; 90% of all exposed areas show severe wear. Only 4% of the exposed areas show mild wear, and 6% show no signs of wear. The distribution is similar for all raceways.

The damage class distribution for $x/2b = 11.44$ and $N = 12500$ can be seen in Figure 18. Most of the exposed areas show severe wear, similar to $x/2b = 2.67$. Overall, 83 % of the exposed areas show severe wear, 3% show mild wear and 14% show no signs of wear. The outer ring shows more severe damages compared to the inner ring. It is noticeable that the Raceway 1 of the inner ring shows 29% undamaged exposed areas.

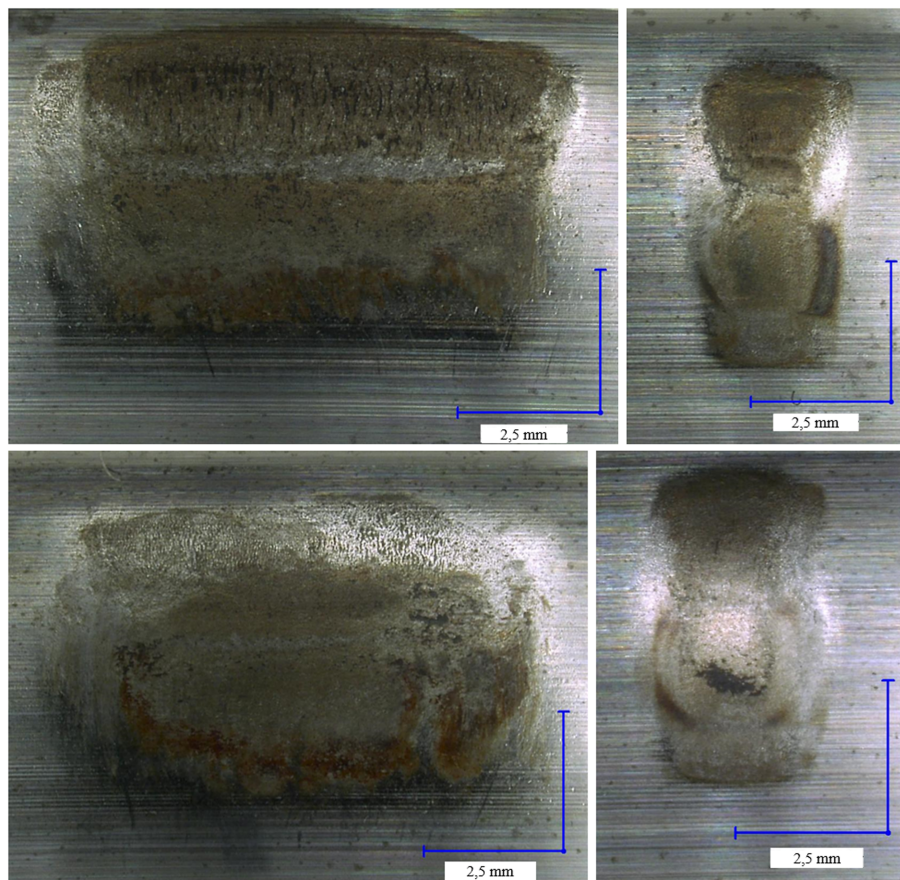


FIGURE 15 Examples of exposed areas with severe wear

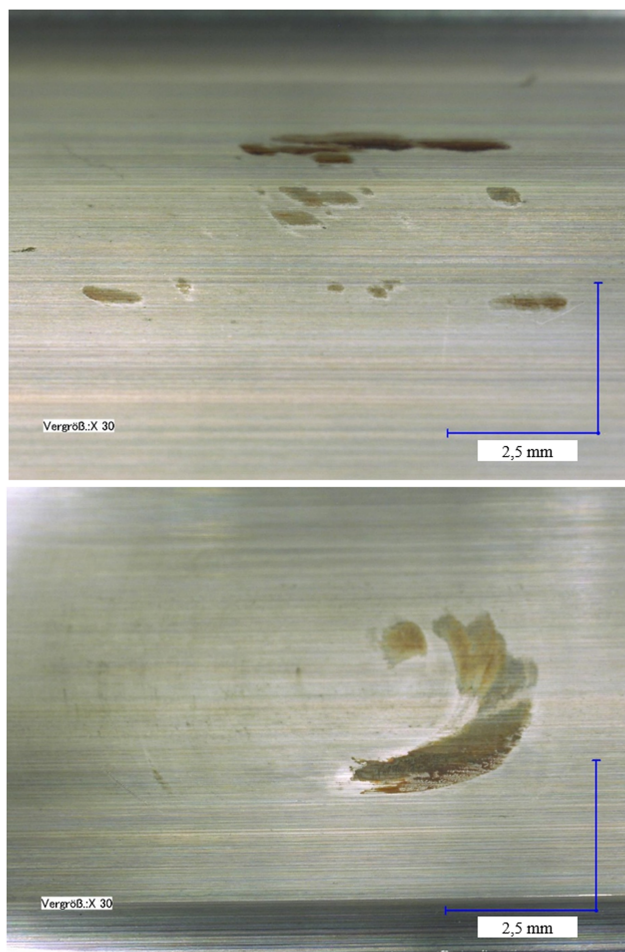


FIGURE 16 Examples of exposed areas with mild wear

Figure 19 shows the distribution for the test with a reduced number of cycles (1250). It can be seen that 13% of the exposed areas show severe wear, 32% show mild wear and 55% show no signs of wear. Due to the lower number of oscillating cycles, it was expected that less wear would occur for this experiment. Nevertheless, the spread between severe, mild and no wear is unexpected since there is no apparent difference in the contact conditions.

The following figures give the location of the damage classes on the bearing rings. The left part shows the inner ring, the centre one the outer ring. Each square is representative of one of the 28 exposed areas per raceway. The colour of the square shows the degree of damage, which can be seen in the legend on the right. In addition, Raceways 1 and 2 are visualized. The black points show the so-called soft spot of the bearing. The raceways are inductively hardened. Furthermore, the rolling elements are mounted with the help of holes in the soft spot. The black arrows show the position of the grease inlets.

The damage occurrence for $x/2b = 2.67$ and $N = 12500$ is shown in Figure 20. Five exposed areas of the inner ring are undamaged. The random distribution of the exposed areas can be justified by the manufacturing process and the position of the lubrication inlets.

The undamaged spots for $x/2b = 11.44$ and $N = 12500$ are randomly distributed, which can again be explained by the manufacturing process and the position of the lubrication inlets; see Figure 21. The load distribution under pure axial load can be affected by the soft spot.⁵⁶ Nevertheless, from the distribution of the wear marks, no pattern affected by the soft spot can be found.

The results for $x/2b = 2.67$ and $N = 1250$ are visualized in Figure 22. It is noticeable here that Raceway 2 for the inner ring shows no major damage, as does Raceway 1 of the outer ring. This leads to the conclusion that damages start on one raceway and evolve to the other raceway.

6.2 | Analyses: T-solid

The T-Solid has a lower number of exposed areas and only one active raceway per row. For $x/2b = 2.67$, the majority of exposed areas show severe wear. Of the inner ring exposed areas, 69% have severe wear, 21% mild wear and 10% no wear. The outer ring had 93% severe wear and

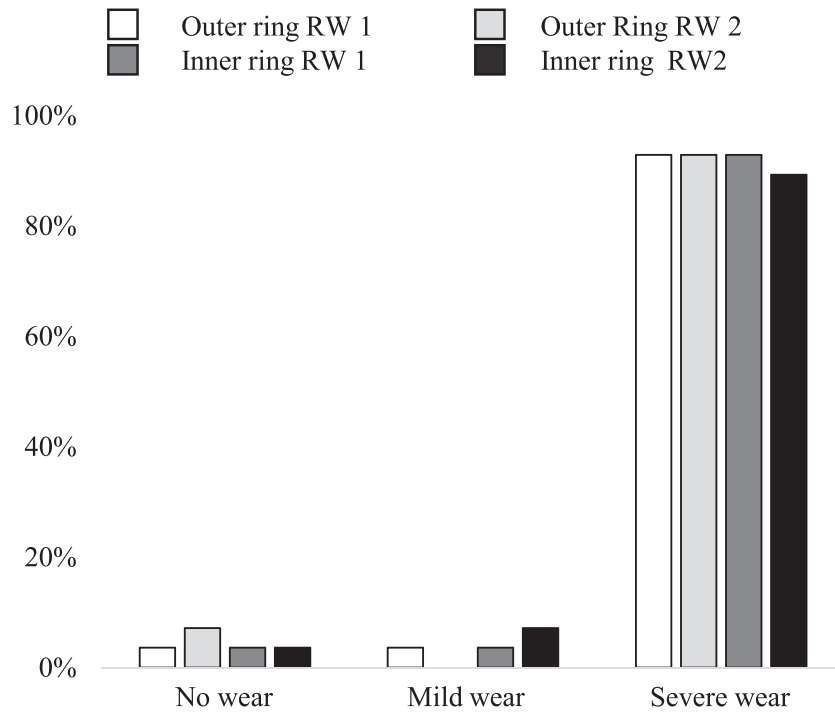


FIGURE 17 Four-point contact ball bearing. Damage class for $x/2b = 2.67$ and $N = 12500$ for Raceways (RWs) 1 and 2

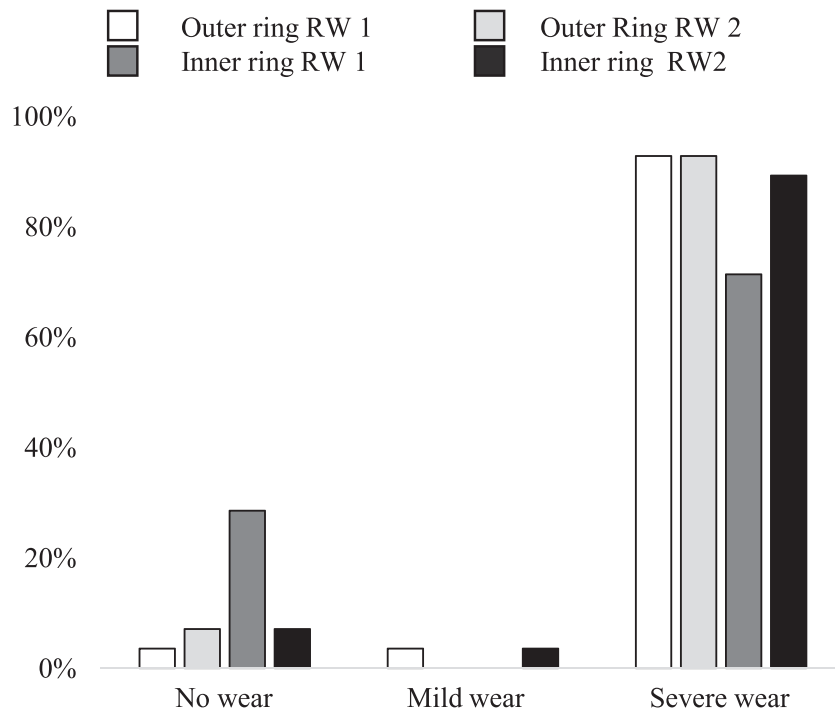


FIGURE 18 Four-point contact ball bearing. Damage class distribution for $x/2b = 11.44$ and $N = 12500$ for Raceways (RWs) 1 and 2

7% mild wear. The results are similar to the four-point contact ball bearing, with a slightly lower fraction of severe wear areas. Figure 23 shows the distribution of damage classes.

For $x/2b = 11.44$, of the exposed areas of the inner ring, 35% show severe damages, 17% mild damages and 48% no damages. For the outer ring, 41% of the exposed areas show severe wear, 31% mild wear and 28% no wear. The distribution is shown in Figure 24. For $x/2b = 11.44$, the T-Solid shows less wear compared to the four-point contact ball bearing.

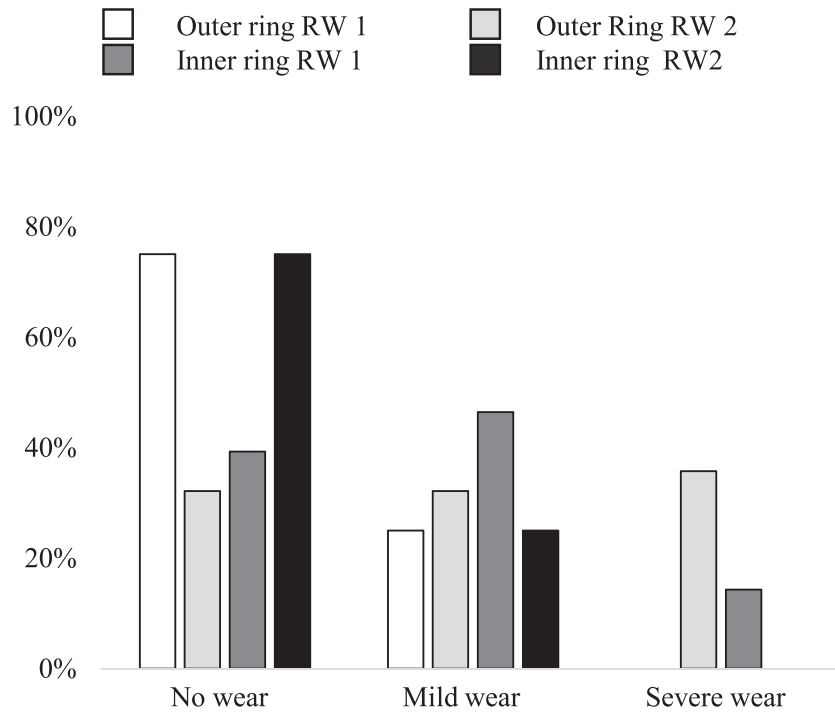


FIGURE 19 Four-point contact ball bearing. Damage class distribution for $x/2b = 2.67$ and $N = 1250$ for Raceways (RWs) 1 and 2

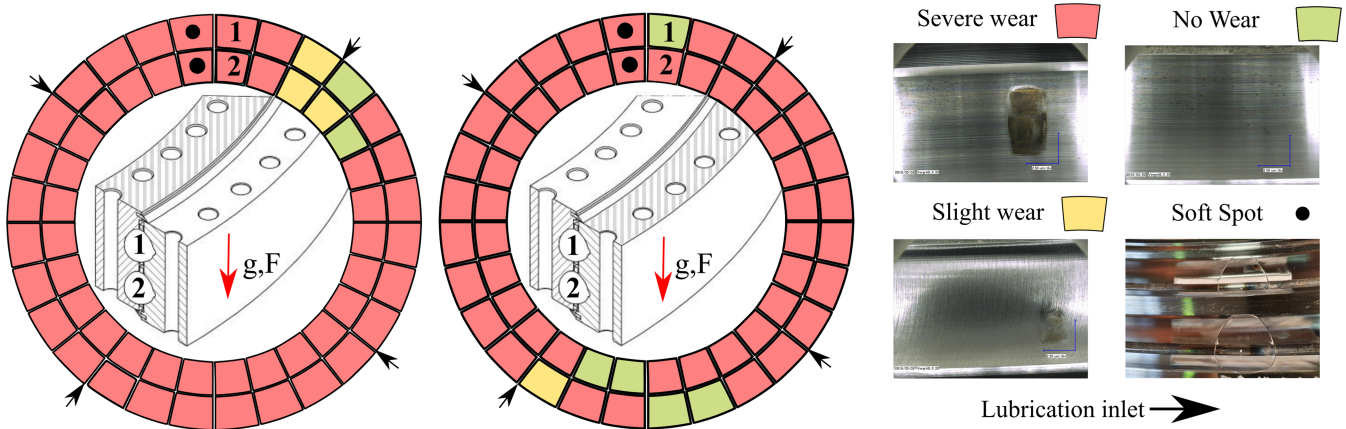


FIGURE 20 Four-point contact ball bearing. Damage class location on raceways for $x/2b = 2.67$ and $N = 12500$

7 | DISCUSSION

The scaling of the test conditions was realized by using similar $x/2b$ ratios, allowing comparison between different ball bearings and ball bearing sizes. The results for angular contact ball bearings of the size 7208 (60-mm pitch diameter)¹⁰ and first results of a four-point contact ball bearing of a 7.5-MW wind turbine (4690-mm pitch diameter)⁵⁷ show similar wear marks to the ones presented in this paper. The comparability of the results is not statistically secured due to the small sample size. The used downscaling process does not consider the total influence of geometry, manufacturing differences and material properties. However, the scaling approach helps to identify trends and critical conditions.

Two different bearing designs were tested under similar conditions. For $x/2b = 2.67$, the results for both bearing types are similar. Both bearing types show primary severe wear marks. Due to the high level of wear, it is not possible to compare the two designs. Nevertheless, the distribution of wear marks differs for the bearing types. For $x/2b = 11.44$, the T-Solid shows less pronounced wear compared to the four-point contact ball bearing. However, the wear level is still high for both designs.

The differences between the wear mark distributions can be explained by several factors, mainly the initial grease lubrication, the guidance behaviour, the ball motion and relative movements in the contact. The initial lubrication for the four-point contact ball bearings was realized

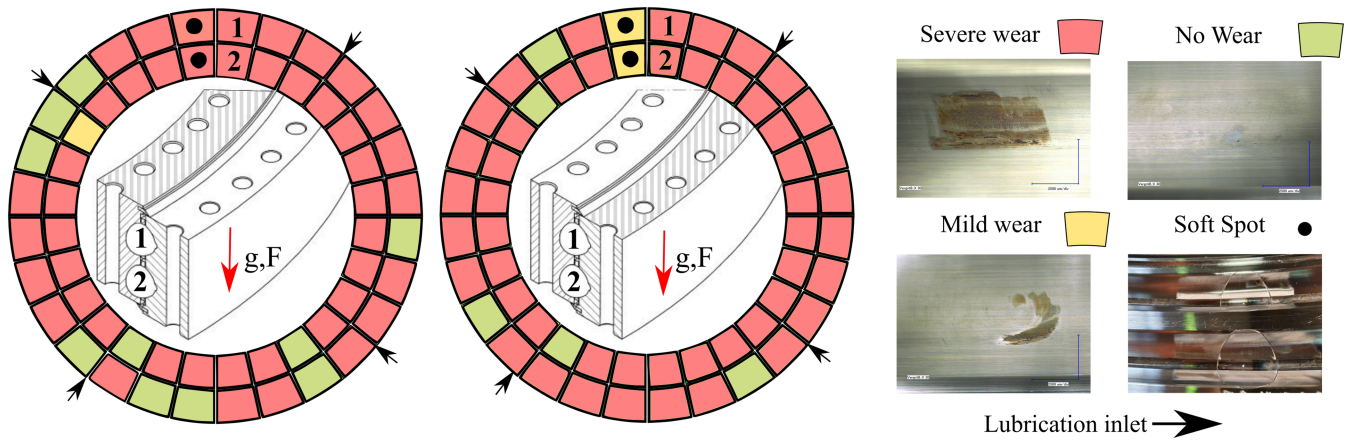


FIGURE 21 Four-point contact ball bearing. Damage class location on raceways for $x/2b = 11.44$ and $N = 12500$

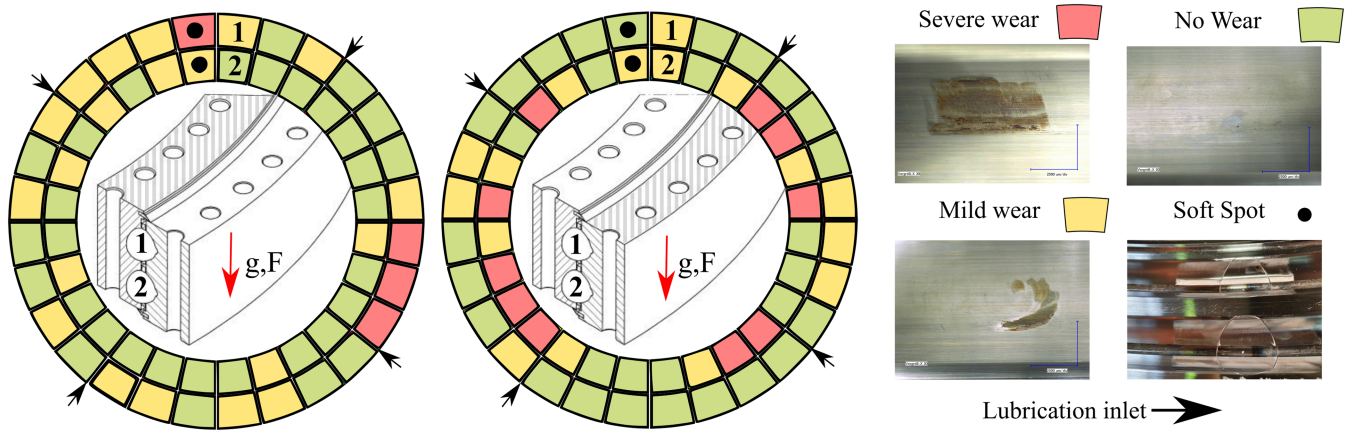


FIGURE 22 Four-point contact ball bearing. Damage class location on raceways for $x/2b = 11.44$ and $N = 1250$

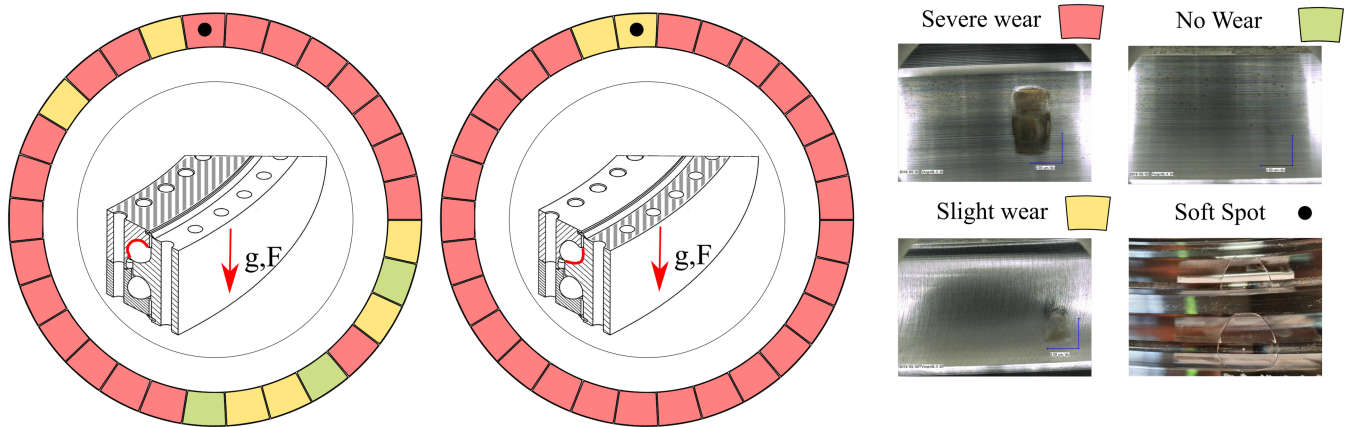


FIGURE 23 T-Solid. Damage class location on raceway for $x/2b=2.67$ and $N = 12500$

through lubrication inlets. The grease distribution was accomplished by rotating the bearing three times. Due to the design of the T-Solid, the grease was applied directly to the raceways. This enabled precise control of the grease distribution, which was not the case with the four-point contact ball bearings. The distributions of damages between the two rows of the four-point bearings do not show a clear pattern. This indicates that gravity did not have a significant effect on grease distribution during the test time. We assume that the influence of the different initial lubrication is comparatively small. The guidance behaviour is improved for closer osculations, which could reduce the level of wear. The closer

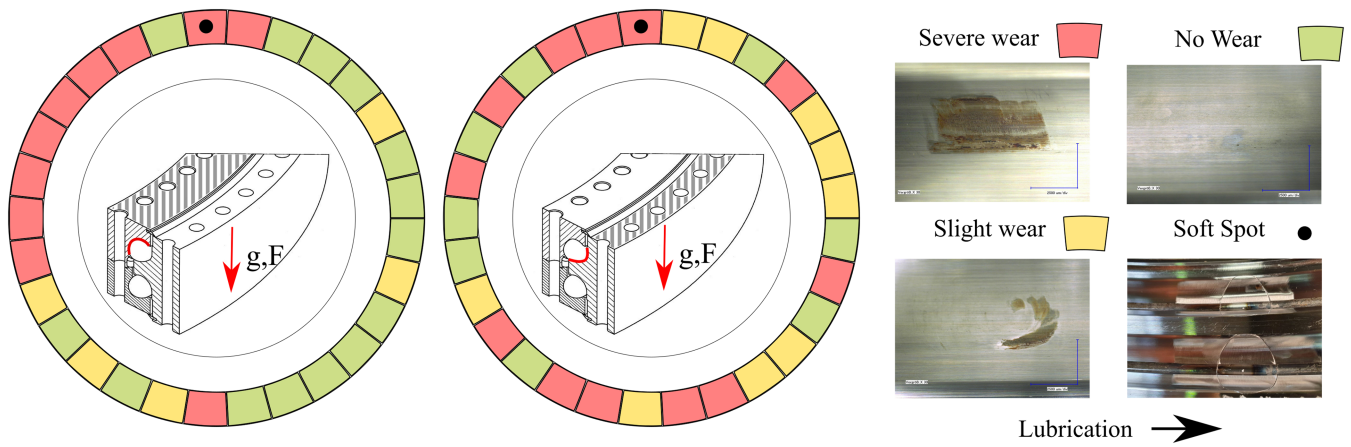


FIGURE 24 T-Solid. Damage class location on raceway for $x/2b = 11.44$ and $N = 12500$

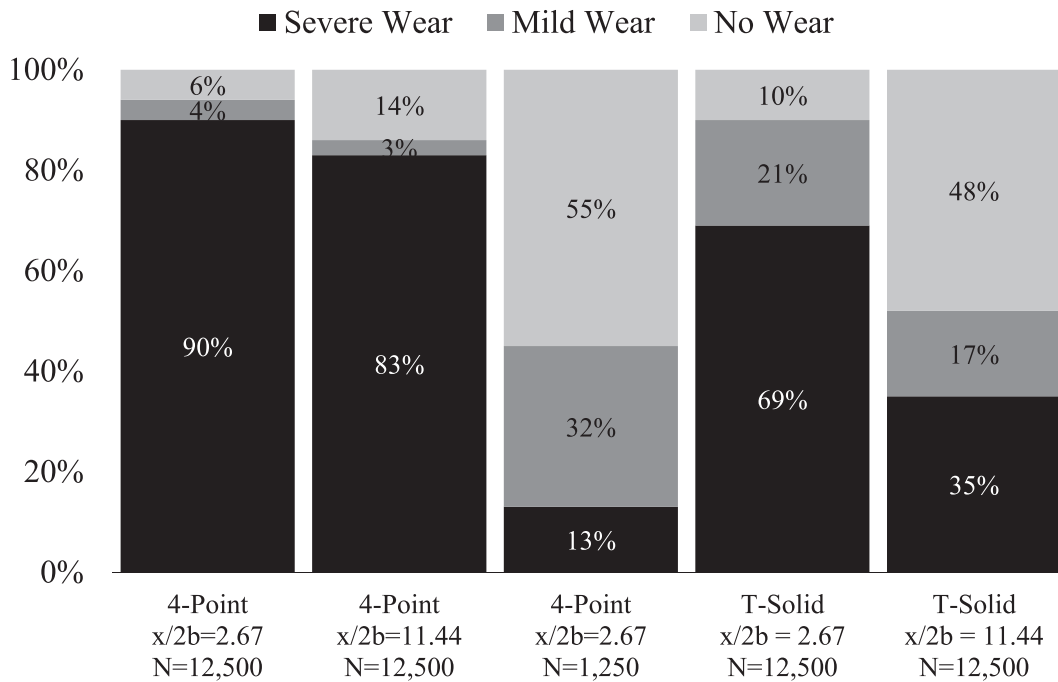


FIGURE 25 Summary of the wear distribution for all experiments

osculation has advantages and disadvantages. The osculation of the T-Solid is 5% closer compared to the four-point contact ball bearing. Both bearing designs use curvature values typical for ball bearings. The closer the osculation, the lower the Hertzian pressure. In our experiments, we made sure that the contact pressure is the same for both types of bearings. A closer osculation also increases the differential slip and, therefore, the friction moment. This can favour the occurrence of wear.⁵¹ More slip can, on the other hand, reduce wear with certain lubricants, as the activation of anti-wear additives requires sliding.^{58,59} Since various combinations of operating conditions occur in the field, the weighting of the various influences can produce results that differ from those shown.

The contact angle affects the frictional work, due to the spin slip that increases with larger angles. Therefore, one would expect that this effect could be seen comparing two bearings with contact angles of 45° and 90° . However, the bigger the diameter of a bearing, the smaller the impact of the spin-slip. Therefore, the minor influence of the spin slip can be explained with the diameter of 750 mm, and it becomes even less apparent in larger pitch bearings. The different slip components (mainly spin and differential slip) were discussed in Schwack et al.⁸ In this paper, a parameter study was presented, in which the dependency between contact angle and frictional work (local sliding multiplied by pressure and coefficient of friction) was shown from an angular contact ball bearing with 80-mm outer diameter.

All bearings displayed damages under all conditions, and it is reasonable to assume that wear under pitch bearing conditions cannot be prevented by any of these ball bearings.

8 | CONCLUSION

Two different bearing designs, a four-point contact ball bearing and a T-Solid bearing, were tested. We tested bearings with an outer diameter of 750 mm. The pitch bearings were tested with $x/2b$ of 2.67 (0.7°) and 11.44 (3.0°). These double amplitudes are typical for oscillations of pitch bearings. Based on aero-elastic simulations and long-term wind speed measurements, the test duration was set to 12 500 cycles. This duration represents the maximum number of cycles without interruption, which is seen as critical for wear development. Supplementary experiments with 1250 cycles investigate typical pitch bearing conditions and early stages of wear.

Both oscillation amplitudes caused severe wear on the majority of exposed areas after 12 500 cycles for both bearing types. Severe wear marks occurred after 1250 cycles as well for the four-point contact ball bearing. The wear marks on the raceways did not prevent the bearings from rotating. Hence, the raceway condition is not critical for a wind turbine application. However, it can be reasoned that further cycles will make the damages worse and can endanger the safe operation of the turbine. Thus, it is recommendable to avoid conditions with sequences of wear-inducing oscillations. Longer pitch movements which interrupt consecutive smaller cycles of the contact are called protection runs and can prevent wear of the raceways.¹² Protection runs may occur by unconscious default, for instance as the turbine's reaction to a wind gust. Otherwise, pro-active setting can be realized without significant power loss.⁶⁰

The experiments with a four-point contact ball bearing showed that for $x/2b = 2.67$ overall 90% and for $x/2b = 11.44$ overall 83% of all exposed areas are severely damaged after 12 500 cycles. For $x/2b = 2.67$ and 1250 cycles, only 13 % of the exposed areas show severe wear. These results are in line with the incubation hypothesis.¹¹

The tests of the T-Solid bearing resulted in less pronounced wear. For $x/2b = 2.67$ the 69% of the exposed areas show severe wear. For $x/2b = 11.44$, 35% of the exposed areas show severe wear. These better results can be due to the initial lubrication directly on the raceway and the better guidance behaviour. Since various combinations of operating conditions occur in the field, the weighting of the various influences can produce results that differ from those shown.

The results of the pitch bearing experiments can be used to develop and improve pitch strategies to reduce wear. In addition, we were able to show the first results of how a change in the bearing design can affect wear; see Figure 25.

ACKNOWLEDGEMENTS

The authors would like to thank the German Federal Ministry for Economy Affairs and Energy (BMWi) for funding the project Highly Accelerated Pitch Bearing Test (HAPT - Project number 0325918) from which this paper originated. They would like to thank Enercon for supplying the wind speed measurement data. Furthermore, the authors would like to thank Felix Prigge for supporting the presented research and the design of the bearing images.

CONFLICT OF INTEREST

The authors declare that they have no conflicts of interest.

AUTHOR CONTRIBUTIONS

Fabian Schwack performed the idea, experiments, evaluation, data curation and writing. Fabian Halmos performed the experiments, evaluation, test rig planning and writing. Matthias Stammler performed the idea, data analysis, project management and writing. Sergei Glavatskih and Gerhard Poll performed the supervision.

PEER REVIEW

The peer review history for this article is available at <https://publons.com/publon/10.1002/we.2693>.

DATA AVAILABILITY STATEMENT

The data that support the findings of this study are available from corresponding authors upon reasonable request.

ORCID

Fabian Schwack  <https://orcid.org/0000-0003-2581-9672>

Matthias Stammler  <https://orcid.org/0000-0003-1874-1344>

Sergei Glavatskih  <https://orcid.org/0000-0002-8738-0047>

REFERENCES

1. Burton T, Sharpe D, Jenkins N, Bossanyi E. *Wind Energy Handbook*. 2nd ed. London: Wiley & Sons; 2012.
2. Bossanyi EA. Individual blade pitch control for load reduction. *Wind Energy*. 2003;6(2):119-128. <https://doi.org/10.1002/we.76>
3. Bossanyi EA. Further load reductions with individual pitch control. *Wind Energy*. 2005;8(4):481-485.
4. Lugt PM. Modern advancements in lubricating grease technology. *Tribol Int*. 2016;97:467-477.
5. Almen JO. Lubricants and false brinelling of ball and roller bearings. *Mech Eng*. 1937;59(6):415-422.
6. Godfrey D. Fretting corrosion or false brinelling? *Tribol Lubr Technol*. 2003;59(12):28-29.
7. Errichello R. Another perspective: False brinelling and fretting corrosion. *Tribol Lubr Technol*. 2004;60:34-36.
8. Schwack F, Prigge F, Poll G. Finite element simulation and experimental analysis of false brinelling and fretting corrosion. *Tribol Int*. 2018;126:352-362. <https://doi.org/10.1016/j.triboint.2018.05.013>
9. Grebe M. False brinelling—standstill marks at roller bearings. *Dissertation*. Bratislava: Faculty of Material Science; 2012.
10. Schwack F, Bader N, Leckner J, Demaille C, Poll G. A study of grease lubricants under wind turbine pitch bearing conditions. *Wear*. 2020;454-455:203335. <https://doi.org/10.1016/j.wear.2020.203335>
11. Schwack F, Byckov A, Bader N, Poll G. Time-dependent analyses of wear in oscillating bearing applications. In: 72th STLE Annual Meeting and Exhibition; 2017; Atlanta, USA.
12. Stammler M, Poll G, Reuter A. The influence of oscillation sequences on rolling bearing wear. *Bearing World J*. 2019;4:19-25.
13. Stammler M, Thomas P, Reuter A, Schwack F, Poll G. Effect of load reduction mechanisms on loads and blade bearing movements of wind turbines. *Wind Energy*. 2020;23:274-290. <https://doi.org/10.1002/we.2428>
14. Chaib Z, Daidié A, Leray D. Screw behavior in large diameter slewing bearing assemblies: numerical and experimental analyses. *Int J Interact Des Manuf (IJIDeM)*. 2007;1(1):21-31. <https://doi.org/10.1007/s12008-007-0003-7>
15. Nam JS, Han JW, Park YJ, Nam YY, Lee GH. Development of highly reproducible test rig for pitch and yaw bearings of wind turbine. *J Mech Sci Technol*. 2014;28(2):705-712. <https://doi.org/10.1007/s12206-013-1134-3>
16. Han JW, Nam JS, Park YJ, Lee GH, Nam YY. An experimental study on the performance and fatigue life of pitch bearing for wind turbine. *J Mech Sci Technol*. 2015;29(5):1963-1971. <https://doi.org/10.1007/s12206-015-0417-2>
17. Liu R, Wang H, Pang BT, Gao XH, Zong HY. Load distribution calculation of a four-point-contact slewing bearing and its experimental verification. *Exp Tech*. 2018;42(3):243-252. <https://doi.org/10.1007/s40799-018-0237-2>
18. Stammler M, Schwack F, Bader N, Reuter A, Poll G. Friction torque of wind-turbine pitch bearings—comparison of experimental results with available models. *Wind Energy Sci*. 2018;3(1):97-105. <https://doi.org/10.5194/wes-3-97-2018>
19. He P, Hong R, Wang H, Lu C. Pitch bearing/raceway fretting: influence of contact angle. *Proc IME B J Eng, Part C J Mech Eng Sci*. 2019;233(5):1734-1749.
20. Popko W. Aero-elastic simulation time series of IWT7.5 reference turbine. In: Fraunhofer Institute for Wind Energy Systems IWES; 2019; Bremerhaven. <https://doi.org/10.24406/fordatis/113>
21. Grebe M, Feinle P, Hunsicker W. Möglichkeiten zur Reduzierung von False Brinelling Schäden. GfT; 2008.
22. Maruyama T, Saitoh T, Yokouchi A. Differences in mechanisms for fretting wear reduction between oil and grease lubrication. *Tribol Trans*. 2017;60(3):497-505. <https://doi.org/10.1080/10402004.2016.1180469>
23. Schadow C. Stillstehende fettgeschmierte Wälzlager unter dynamischer Beanspruchung. *Dissertation*. Magdeburg: Lehrstuhl für Maschinenelemente und Tribologie; 2016.
24. Frache L, Komba EH, Philippon D, et al. Observation of a modified superficial layer on heavily loaded contacts under grease lubrication. *Tribol Int*. 2021;158:106921. <https://doi.org/10.1016/j.triboint.2021.106921>
25. Brockley CA. The wear characteristics of the oscillating bearing. *Wear*. 1961;4(5):333-344. [https://doi.org/10.1016/0043-1648\(61\)90001-1](https://doi.org/10.1016/0043-1648(61)90001-1)
26. Berthier Y, Play D. Wear control of cylindrical dry oscillating bearings. In: Developments in Numerical and Experimental Methods Applied to Tribology. Proceedings of the 10th Leeds-Lyon Symposium on Tribology, Lyon, France, 6-9 September 1983. Butterworths; 1984:187-196. <https://doi.org/10.1016/B978-0-408-22164-1.50031-4>
27. Berthier Y, Play D. Wear mechanisms in oscillating bearings. *Wear*. 1989;75:369-387. [https://doi.org/10.1016/0043-1648\(82\)90159-4](https://doi.org/10.1016/0043-1648(82)90159-4)
28. Ghezzi I, Komba EWH, Tonazzi D, Bouscharain N, Le Jeune G, Coudert JB, Massi F. Damage evolution and contact surfaces analysis of high-loaded oscillating hybrid bearings. *Wear*. 2018;406:1-12. <https://doi.org/10.1016/j.wear.2018.03.016>
29. Fallahnezhad K, Brinji O, Desai A, Meehan PA. The influence of different types of loading on false brinelling. *Wear*. 2019;440:203097. <https://doi.org/10.1016/j.wear.2019.203097>
30. Fallahnezhad K, Liu S, Brinji O, Marker M, Meehan PA. Monitoring and modelling of false brinelling for railway bearings. *Wear*. 2019;424:151-164. <https://doi.org/10.1016/j.wear.2019.02.004>
31. Schwack F, Schneider V, Wandel S, de la Presilla RJ, Poll G, Glavatskih S. On the critical amplitude in oscillating rolling element bearings. *Tribol Int*; 163:107154.
32. Gänsheimer J, Friedrich G. Testing machines to study fretting wear. *Wear*. 1971;17(5-6):407-419.
33. Zhu MH, Zhou ZR. On the mechanisms of various fretting wear modes. *Tribol Int*. 2011;44(11):1378-1388.
34. Harris T, Rumbarger JH, Butterfield CP. Wind turbine design guideline dg03: Yaw and pitch rolling bearing life: Technical report. NREL/TP-500-42362NREL; 2009.
35. Houpert L. Bearing life calculation in oscillatory applications©. *Tribol Trans*. 1999;42:136-143. <https://doi.org/10.1080/10402009908982200>
36. Schwack F, Stammler M, Flory H, Poll G. Free contact angles in pitch bearings and their impact on contact and stress conditions. In: European Wind Energy Association; 2016; Hamburg, Germany.
37. Wöll L, Jacobs G, Kramer A. Lifetime calculation of irregularly oscillating bearings in offshore winches. *Model Identif Control*. 2018;39(2):61-72.
38. Menck O, Stammler M, Schleich F. Fatigue lifetime calculation of wind turbine blade bearings considering blade-dependent load distribution. *Wind Energy Sci*. 2020;5(4):1743-1754.
39. Popko W, Thomas P, Sevinc A, et al. IWES Wind Turbine IWT-7.5-164 Rev. 4. In: Fraunhofer Institute for Wind Energy Systems IWES; 2018; Bremerhaven. <https://doi.org/10.24406/IWES-N-518562>
40. Guideline for the certification of wind turbines; 2010.

41. Fingersh L, Hand M, Laxson A. Wind turbine design cost and scaling model, Golden, CO (United States): National Renewable Energy Laboratory; 2006.
42. Harris TA, Kotzalas MN. *Rolling Bearing Analysis*. 5th ed.: CRC, Taylor & Francis; 2007.
43. Juettner M, Hasse A, Tremmel S. Flexure pitch bearing concept for individual pitch control of wind turbines. *Wind Energy*. 2018;21(2):129-138. <https://doi.org/10.1002/we.2149>
44. de Vries E. Pitch bearing breakthrough. *Wind Power Monthly*. 2014. <https://www.windpowermonthly.com/article/1309620/pitch-bearing-breakthrough>
45. Schwack F, Stammler M, Poll G, Reuter A. Comparison of life calculations for oscillating bearings considering individual pitch control in wind turbines. *J Phys Conf Ser*. 2016;753:112013. <https://doi.org/10.1088/1742-6596/753/11/112013>
46. Daidie A, Chaib Z, Ghosn A. 3D simplified finite elements analysis of load and contact angle in a slewing ball bearing. *ASLE Trans*. 2008;130(8). <https://doi.org/10.1115/1.2918915>
47. Chen L, Zhang X. Contact stress and deformation of blade bearing in wind turbine. *International Conference on Measuring Technology and Mechatronics Automation*. Changsha, China: IEEE; 2010:833-836.
48. Chen G, Wen J. Load performance of large-scale rolling bearings with supporting structure in wind turbines. *J Tribol*. 2012;134:41105. <https://doi.org/10.1115/1.4007349>
49. Kingsbury EP. Precessional slip in an angular contact ball bearing. *Wear*. 1982;77(1):105-114.
50. Kingsbury E. Pivoting and slip in an angular contact bearing. *ASLE Trans*. 1984;27(3):259-262.
51. Shima M, Qijun L, Aihara S, Yamamoto T, Sato J, Waterhouse RB. Design effects on the fretting wear behaviour of ball bearings. *Tribol Int*. 1997; 30(10):773-778.
52. Stammler M, Reuter A, Poll G. Cycle counting of roller bearing oscillations—case study of wind turbine individual pitching system. *Renew Energy Focus*. 2018;25:40-47. <https://doi.org/10.1016/j.ref.2018.02.004>
53. Hertz HR. Über die berührung fester elastischer körper. *J für die reine Angew Math*. 1881;92:156-171.
54. Song W, Karikari-Boateng KA, Lee H. Pitch bearing case study with supervisory control data of 7mw wind turbine. *Developments in renewable energies offshore*: CRC Press; 2020:515-524.
55. Song W, Karikari-Boateng KA. Enhanced test strategy of pitch bearing based on detailed motion profile. *Forsch Ingenieurwes*. 2021:1-11.
56. Gui JX, Wang GB, Zhou Z. Load Analysis of pitch bearing considering non-quenching zone. *Vibroengineering Procedia*. 2019;25:7-12. <https://doi.org/10.21595/vp.2019.20704>
57. Stammler M. Endurance test strategies for pitch bearings of wind turbines. Ph.D. Thesis; 2020.
58. Spikes H. The history and mechanisms of zddp. *Tribol Lett*. 2004;17(3):469-489.
59. Zhang J, Spikes H. On the mechanism of zddp antiwear film formation. *Tribol Lett*. 2016;63(2):1-15.
60. Schwack F, Stammler M, Bartschat A, Pape F & Poll G. Solutions to reduce wear in wind turbine blade bearings. 2018;3.

How to cite this article: Schwack F, Halmos F, Stammler M, Poll G, Glavatskih S. Wear in wind turbine pitch bearings—A comparative design study. *Wind Energy*. 2022;25(4):700-718. doi:10.1002/we.2693